NEUTRON BACKGROUND AT BOULBY MINE

V. A. KUDRYAVTSEV, P. K. LIGHTFOOT, J. E. MCMILLAN,
M. ROBINSON AND N. J. C. SPOONER
Department of Physics and Astronomy, University of Sheffield, Sheffield, S3 7RH, UK

P. F. SMITH, N. J. T. SMITH AND J. D. LEWIN
Particle Physics Department, Rutherford Appleton Laboratory, Chilton, Oxon OX11 0QX, UK

R. LÜSCHER AND I. LIUBARSKY
Blackett Laboratory, Imperial College of Science, Technology and Medicine, London SW7 2BZ, UK

The neutron background at the underground laboratory at Boulby - a site for several dark matter experiments - is discussed. Special emphasis is put on the neutron background produced by cosmic-ray muons. The most recent versions of the muon propagation code MUSIC, and particle transport code FLUKA are used to evaluate muon and neutron fluxes. The results of simulations are compared with experimental data.

1. Introduction

Neutrons are the major background in experiments searching for WIMP dark matter particles – also known as neutralinos. WIMPs are expected to interact with ordinary matter in detectors to produce nuclear recoils, which can be detected through ionisation, scintillation or phonons. Identical events can be induced by neutrons. Thus, only suppression of any background neutron flux by passive or active shielding will allow experiments to reach sufficiently high sensitivity to neutralinos. Designing shielding for such detectors requires simulation of neutron fluxes.

Neutrons underground arise from two sources: i) local radioactivity, and ii) cosmic-ray muons. Neutrons associated with local radioactivity are produced mainly via (α, n) reactions, initiated by α-particles from U/Th traces in the rock and detector elements. Neutrons from spontaneous fission of ^{238}U contribute also to the flux at low energies. The neutron yield

from cosmic-ray muons depends strongly on the depth of the underground laboratory. At Boulby it is about 3 orders of magnitude less than that of neutrons arising from local radioactivity. A larger thickness of rock suppresses the muon flux and, hence, reduces also the neutron yield. The dependence, however, is not linear. The muon-induced neutron flux can be important for experiments intending to reach high sensitivity to WIMPs or to low-energy neutrino fluxes. There are several reasons for this: 1) the energy spectrum of muon-induced neutrons is hard, extending to GeV energies, and fast neutrons can travel far from the associated muon track, reaching a detector from large distances; 2) fast neutrons transfer larger energies to nuclear recoils making them visible in dark matter detectors, while many recoils from α-induced neutrons fall below detector energy thresholds; 3) a detector can be protected against neutrons from the rock activity by hydrogen-rich material, possibly with addition of thermal neutron absorber; such a material, however, will be a target for cosmic-ray muons and will not protect against muon-induced neutrons. The only way to reduce this flux is to add an active muon and/or neutron veto (see also Ref. [1] for discussion).

2. Neutrons from the radioactivity in Boulby rock

Several samples of rock in the Boulby mine around the experimental labs (mainly halite) were used to measure the contamination of U and Th. It was found that the fractions of these elements do not exceed 60 ppb of U and 300 ppb of Th, but show large variations from sample to sample, being on average about 30 ppb of U and 150 ppb of Th. This gives about 2×10^{-8} neutrons/g/s in halite. Neutron propagation with MCNP [2] results in a preliminary estimate of the neutron flux behind the lead (15 cm) and copper (10 cm) shielding of about 10^{-6} cm^{-2} s^{-1} above 100 keV. Figure 1 shows the absorption of the flux as a function of the thickness of the CH_2 material, commonly used to shield detectors from neutrons. 10 cm of CH_2 suppresses the neutron flux from the rock by about one order of magnitude.

3. Muon flux and energy spectrum underground

Knowledge of the muon flux is clearly important for calculations of the muon-induced neutron flux or counting rate – it provides the absolute normalisation. The muon energy spectrum at a given experimental site also affects the neutron production rate. Thus precise knowledge of the muon spectrum and absolute normalisation is crucial for neutron flux simulations.

The measurement of the muon flux at Boulby was carried out using the liquid scintillator veto system of the ZEPLIN I dark matter detector [3].

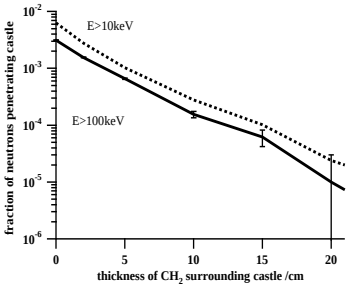

Figure 1. Fraction of survived neutrons above 10 keV and 100 keV as a function of CH_2 thickness (behind 15 cm of lead and 10 cm of copper).

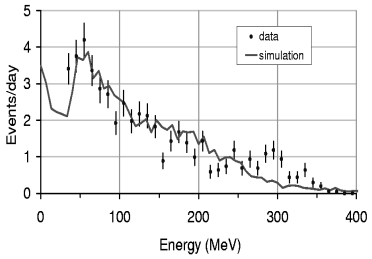

Figure 2. Muon energy deposition spectrum: measurements (filled circles and simulations (solid curve)

The details of the experiment are described in Ref. [4]. Figure 2 shows the spectrum of energy depositions compared with the normalised simulated spectrum. The simulations of muons were performed taking into account the calculated underground muon flux and energy spectrum in Boulby rock, the detector geometry, the muon energy losses due to ionisation and the propagation of scintillation photons in the detector. The calculations of the muon fluxes and energy spectra at various depths in Boulby rock were done using the parameterisation of the muon spectrum at the surface [5] and the muon propagation code MUSIC [6] (see also Refs. [4,7] for more details).

The simulations were then used to convert the measured muon rate in the detector to the muon flux, which was found to be $(4.09 \pm 0.15) \times 10^{-8}$ cm^{-2} s^{-1}, where the error includes both statistical and systematic uncertainties, the latter being due to the applied cuts, uncertainties in the energy threshold, energy calibration etc. The comparison between measured and simulated fluxes provides an estimate of the rock overburden (column density at vertical), which is 2805±45 m w. e. assuming a flat surface above the detector. The error in depth includes the uncertainties in the flux measurements, as well as in the rock composition.

4. Simulations of muon-induced neutrons

The neutron production by muons and neutron transport were simulated with FLUKA [8]. The average number of neutrons produced by a muon per unit path length (1 g/cm^2) in scintillator is presented in Figure 3 as a function of muon energy. Our results (filled circles) have been fitted to a function $R_n = a \times E^{\alpha}$, where $a = (3.20 \pm 0.10) \times 10^{-6}$ and $\alpha = 0.79 \pm 0.01$.

This is consistent with FLUKA simulations by Wang et al. [9] (dashed line). Also shown in Figure 3 are measurements of neutron production by several experiments (open circles with error bars). Their results are plotted as a function of mean muon energy for these experiments (see Ref. [7] for details).

The simulated neutron production by muons with a real spectrum for depths of 0.55 km w.e. and 3 km w.e. in Boulby rock (mean energies 98 and 264 GeV, respectively) is shown by filled squares (below the solid line) in Figure 3. In both cases a smaller neutron production rate was found. The difference is of the order of (10-15)%. A similar difference was found also for muon production in NaCl salt – the result is relevant to the neutron background in salt mines and other rocks.

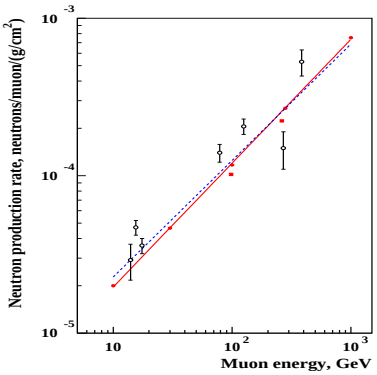

Figure 3. Average number of neutrons produced by a muon per unit path length (1 g/cm^2) in scintillator as a function of muon energy. See text for details.

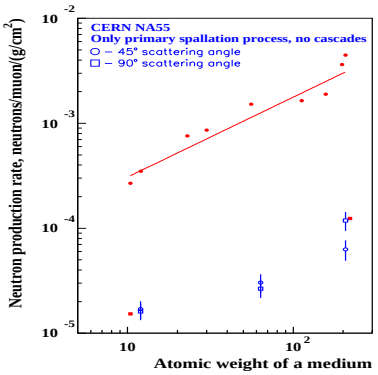

Figure 4. Dependence of neutron rate on the atomic weight of material. For the muon spallation our result for lead is shifted to A=220 to avoid the overlaping with the CERN point.

We studied also the dependence of neutron rate on the atomic weight of material. The neutron rate was obtained with 280 GeV muons in several materials and compounds and is shown in Figure 4 by filled circles. It is obvious that on average the neutron rate increases with the atomic weight of material, but no exact parameterisation was found, which would explain the behaviour for all elements and/or compounds. The general trend can be fitted by a simple power-law form (solid line in Figure 4) $R_n = b \times A^{\beta}$, where $b = (5.33 \pm 0.17) \times 10^{-5}$, A is the atomic weight (or mean atomic weight in the case of a compound) and $\beta = 0.76 \pm 0.01$. We compared our results with measurements performed in the NA55 experiment at CERN with a 190 GeV muon beam [10]. The neutron production was measured in thin targets at several neutron scattering angles, so direct comparison

with our simulations is difficult. The use of thin targets allowed the measurement of neutron production in the first muon interaction only (without accounting for neutrons produced in cascades) [10]. We calculated neutron production in the first muon interaction in scintillator and lead and plotted it in Figure 4 (filled squares) together with the measurements [10] at two scattering angles (open circles and open squares). Since the measured values refer to particular scattering angles, we normalised them to our results at small atomic weight (carbon). The measured behaviour of the neutron rate with atomic weight agrees well with FLUKA predictions.

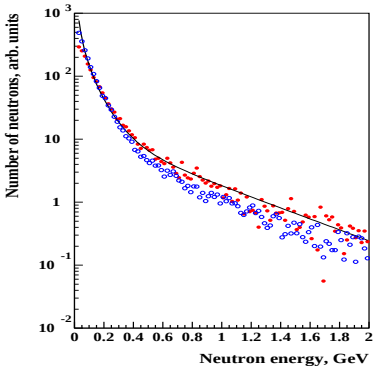

Figure 5. Neutron energy spectrum in scintillator (filled circles) and NaCl (open circles).

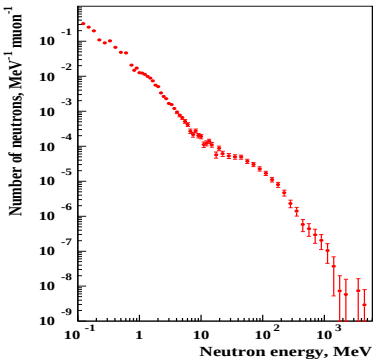

Figure 6. Neutron energy spectrum at the boundary between salt and cavern.

The neutron energy spectrum was calculated for various targets. Figure 5 shows the spectrum obtained for scintillator and NaCl together with parameterisation proposed for scintillator and 280 GeV muons in Ref. [9] (solid curve with arbitrary normalisation). In our simulations the real muon spectrum at about 3 km w.e. underground was used. The neutron energy spectrum becomes softer with increase of $< A >$, although the total neutron production rate increases (see Figure 4).

The simulation of the energy spectrum of neutrons coming from the rock (NaCl) into the laboratory hall or cavern was carried out with the real muon energy spectrum for Boulby. The volume of the salt region was taken as $20 \times 20 \times 20$ m^3, with the cavern for the detector of size $6 \times 6 \times 5$ m^3. The neutrons in the simulations did not stop in the cavern but were propagated to the opposite wall where they could be scattered back into the cavern and could be counted again. Figure 6 shows the simulated neutron energy spectrum at the salt/cavern boundary. If the neutrons entering the cavern for the first time are absorbed in the simulations (cannot be scattered back

from the walls and are counted only once), then the flux below 1 MeV is 2-3 times lower than that shown in Figure 6, in good agreement with the simulations of neutron propagation by Smith [11]. At high energies the flux does not change much. To obtain the neutron flux in units MeV^{-1} cm^{-2} s^{-1} the differential spectrum plotted on Figure 6 has to be multiplied by the muon flux. The total number of neutrons entering the cavern is about 5.8×10^{-10} cm^{-2} s^{-1} above 1 MeV at 3 km w. e. in Boulby rock. The flux on an actual detector can be different from the flux on the boundary salt/cavern due to the interactions of neutrons in the detector itself.

5. Conclusions

We have discussed neutron background, in particular muon-induced neutron background relevant to dark matter experiments. Neutron production by cosmic-ray muons was simulated for various muon energies and various materials. We found reasonably good agreement with the recent experimental data. Our simulation is the starting point of a three-dimensional Monte Carlo to study the neutron background for any detector.

Acknowledgments

We wish to thank PPARC for financial support. We are also grateful to the UKDMC and to the staff of Cleveland Potash Ltd for technical assistance. P. F. Smith acknowledges support from an Emeritus Research Award by the Leverhulme Trust.

References

1. A. S. Murphy, P. F. Smith and D. Snowden-Ifft, these Proceedings.
2. MCNP-4B, Technical Report LA-12625-M (Ed. J. F. Briesmeister), Los Alamos, 1997.
3. N. J. T. Smith et al., these Proceedings.
4. M. Robinson et al., submitted to *Nucl. Instrum. Meth. Phys. Res. A*.
5. M. Aglietta et al. (LVD Collaboration), *Phys. Rev. D*, **58**, 092005 (1998).
6. P. Antonioli, C. Ghetti, E. V. Korolkova, V. A. Kudryavtsev, and G. Sartorelli, *Astroparticle Physics*, **7**, 357 (1997).
7. V. A. Kudryavtsev et al. submitted to *Nucl. Instrum. Meth. Phys. Res. A*.
8. A. Fassò, A. Ferrari, P. R. Sala. *Proceedings of the MonteCarlo 2000 Conference* (Lisbon, October 23-26, 2000), Ed. A.Kling et al. (Springer-Verlag, Berlin, 2001), p. 159; A. Fassò, A. Ferrari, J. Ranft, P. R. Sala, *ibid.* p. 995.
9. Y.-F. Wang et al. *Phys. Rev. D*, **64**, 013012 (2001).
10. V. Chazal et al. *Nucl. Instrum. Meth. Phys. Res. A*, **490**, 334 (2002).
11. P. F. Smith. *Astroparticle Phys.*, **8**, 27 (1997); *Astroparticle Phys.*, **16**, 75 (2001).